

Memo2496: Expert-Annotated Dataset and Dual-View Adaptive Framework for Music Emotion Recognition

Qilin Li , *Student Member, IEEE*, C. L. Philip Chen , *Life Fellow, IEEE*, Tong Zhang , *Senior Member, IEEE*,

Abstract—Music Emotion Recogniser (MER) research faces challenges due to limited high-quality annotated datasets and difficulties in addressing cross-track feature drift. This work presents two primary contributions to address these issues. Memo2496, a large-scale dataset, offers 2496 instrumental music tracks with continuous valence arousal labels, annotated by 30 certified music specialists. Annotation quality is ensured through calibration with extreme emotion exemplars and a consistency threshold of 0.25, measured by Euclidean distance in the valence arousal space. Furthermore, the Dual-view Adaptive Music Emotion Recogniser (DAMER) is introduced. DAMER integrates three synergistic modules: Dual Stream Attention Fusion (DSAF) facilitates token-level bidirectional interaction between Mel spectrograms and cochleograms via cross attention mechanisms; Progressive Confidence Labelling (PCL) generates reliable pseudo labels employing curriculum-based temperature scheduling and consistency quantification using Jensen Shannon divergence; and Style Anchored Memory Learning (SAML) maintains a contrastive memory queue to mitigate cross-track feature drift. Extensive experiments on the Memo2496, 1000songs, and PMEMo datasets demonstrate DAMER’s state-of-the-art performance, improving arousal dimension accuracy by 3.43%, 2.25%, and 0.17%, respectively. Ablation studies and visualisation analyses validate each module’s contribution. Both the dataset and source code are publicly available.

Index Terms—Music emotion recognition, affective computing, dual-view learning, cross-attention fusion, pseudo-label learning, contrastive memory, expert-annotated dataset

I. INTRODUCTION

MUSIC Emotion Recognition (MER), a pivotal domain within affective computing, addresses the challenge of automatically identifying and quantifying emotional content

This work was funded in part by the National Natural Science Foundation of China grant under number 62222603, in part by the STI2030-Major Projects grant from the Ministry of Science and Technology of the People’s Republic of China under number 2021ZD0200700, in part by the Key-Area Research and Development Program of Guangdong Province under number 2023B0303030001, in part by the Program for Guangdong Introducing Innovative and Entrepreneurial Teams (2019ZT08X214), and in part by the Science and Technology Program of Guangzhou under number 2024A04J6310.

Qilin Li, C. L. Philip Chen and Tong Zhang are with the Guangdong Provincial Key Laboratory of AI Large Model and Intelligent Cognition, the School of Computer Science and Engineering, South China University of Technology, Guangzhou 510006, China, and with Research Centre for AI Large Models and Intelligent Cognition, Pazhou Lab, Guangzhou 510335, China, and also with Engineering Research Centre of the Ministry of Education on Health Intelligent Perception and Paralleled Digital-Human, South China University of Technology, Guangzhou 510006, China.

Tong Zhang is the corresponding author (e-mail: tony@scut.edu.cn).

Dataset and code are available at figshare via Music Emotion Dataset with 2496 Songs for Music Emotion Recognition (Memo2496).

conveyed or evoked by musical stimuli [1], [2]. Distinguished from speech or visual emotion recognition, MER encapsulates affective information hierarchically, from micro-level acoustic features to macro-level compositional elements. This presents unique modelling challenges, necessitating sophisticated temporal and multimodal processing strategies [3], [4]. MER finds widespread application in personalised music recommendations, mental health interventions, immersive entertainment, and market analysis [5]–[9]. Positioned across music information retrieval, signal processing, machine learning, and cognitive science, MER’s methodological progression—from handcrafted feature extraction to end-to-end deep representation learning and multimodal fusion—mirrors broader trends in affective computing, rendering its advances transferable to adjacent domains.

MER faces fundamental challenges constraining its generalisability and deployment [10]. Annotation subjectivity, stemming from individual differences, creates a ‘ground-truth ceiling,’ complicating MER evaluation [11], [12]. Cross-cultural and genre-specific domain shifts further invalidate universal emotion-music mappings [13]; cognitive heterogeneity necessitates personalised models [14], [15]. Existing datasets are limited, imbalanced, and inconsistently annotated, with varied temporal granularities impeding cross-corpus comparability. Addressing these issues requires uncertainty-aware annotation fusion for subjective data, robust domain adaptation for cross-domain variability, and culturally inclusive, large-scale datasets.

The scarcity and inherent limitations of existing MER datasets significantly impede algorithmic progress and undermine the ecological validity of findings [16], [17]. Widely adopted corpora, such as the 1000 Songs Database and AMG1608, often rely on crowdsourced annotations [18], [19]. While enabling rapid data collection, this approach tends to introduce systematic noise and inter-annotator disagreement, primarily due to the limited musicological expertise of non-expert annotators, thereby compromising the generalisability and reliability of research outcomes. Beyond annotation quality, existing datasets frequently exhibit substantial limitations in scale and scope. For instance, PMEMo and EMOPIA are relatively small and stylistically restricted, often focusing on compositions such as pop piano pieces, which may prove insufficient for deep neural models that demand large, diverse datasets for effective generalisation [17], [20], [21]. Furthermore, VGMDI displays a notable genre bias

towards music for interactive media [22]. Such fragmentation impedes the development of generalisable models and their broad applicability. Consequently, the field lacks a large-scale, expertly annotated collection of purely instrumental music, encompassing diverse genres, cultures, and eras, complete with fine-grained temporal emotion annotations and rigorous inter-annotator agreement protocols [21]. This deficit compels researchers either to train models on small, homogeneous corpora that may overfit to specific niches, or to aggregate heterogeneous datasets with incompatible annotation schemes [19]. Both approaches compromise model reliability and hinder meaningful cross-study comparisons.

Methodological limitations persist in MER. Unimodal acoustic features, even physiologically augmented, offer negligible performance given their computational burden and inadequately capture semantic richness or disambiguate emotionally divergent passages [23]–[26]. semi-supervised Learning SSL paradigms, relying on pseudo labelling, assign hard labels without uncertainty, propagating noise and biases; they also neglect class imbalance, temporal dynamics and domain specific emotion semantics, causing suboptimal pseudo label quality and diminished robustness across diverse data [27], [28]. cross-track and cross genre feature drift challenges models, degrading performance on heterogeneous distributions [29]. Domain adaptation techniques, though existing [30], are limited in MER as transfer learning presumes labelled target domain data, which are rarely available. Such shortcomings necessitate integrated multimodal architectures incorporating uncertainty aware pseudo labelling, principled domain adaptation and robust feature representations to disentangle emotion relevant invariances from genre specific confounds.

A comprehensive framework for music emotion recognition is presented, which includes a large-scale expert-annotated dataset and a novel dual-view adaptive learning method. This approach addresses critical challenges in Music Emotion Recognition, specifically the limited availability of high-quality annotated data, suboptimal fusion of complementary acoustic features, and performance degradation due to cross-track style drift. To mitigate these challenges, Memo2496 provides an expert-annotated dataset addressing data scarcity, while the Dual-view Adaptive Music Emotion Recogniser (DAMER) offers innovative solutions for feature fusion, pseudo-labelling, and style drift. The principal contributions are summarised below:

- 1) The Memo2496 dataset, comprising 2496 music tracks with continuous Valence–Arousal (V–A) labels, ensures annotation reliability through a V–A consistency threshold.
- 2) A Dual-View Adaptive Framework (DAMER) employs a Dual-Stream Attention Fusion (DSAF) module, fusing Mel spectrograms and cochleograms via bidirectional cross-attention for interaction.
- 3) A Progressive Confidence Labeling (PCL) module enhances pseudo-label reliability and mitigates data scarcity by quantifying prediction consistency and employing an adaptive curriculum-based strategy to generate high-quality pseudo-labels, mitigating the impact of noisy labels.

- 4) Cross-track style drift, defined as performance degradation from stylistic variations, is addressed by a Style-Anchored Memory Learning (SAML) module. SAML maintains a sliding feature queue and employs supervised contrastive loss, anchoring samples sharing the same emotion class while separating heterogeneous styles.

II. RELATED WORK

A. Music Emotion Datasets

Initial MER datasets, while establishing evaluation benchmarks, encounter methodological constraints from copyright and annotation costs [35]. The MIREX Audio Mood Classification task pioneers community evaluation protocols. Its rigid, discrete five-cluster taxonomy, however, lacks psychological grounding, thereby restricting cross-study comparability and capturing only limited affective experience [35]. Subsequently, the 1000 Songs Database addresses copyright and scale limitations through crowdsourced V-A annotations from the Free Music Archive, establishing the dimensional approach as a dominant MER paradigm [31], [32]. Building upon this, AMG1608 extends the V-A framework to 1,608 30-second excerpts with continuous frame-level annotations. However, non-expert crowdworker reliance results in moderate inter-annotator agreement and variable emotional competence [32], [34]. These initiatives confront an inherent trade-off: Creative Commons-licensed music provides accessibility and reproducibility, yet its genre biases towards independent productions constrain generalisability to mainstream music prevalent in real-world listening contexts.

Existing music emotion recognition MER datasets, such as multimodal PMEmo [36] and piano-centric EMOPIA [17], often present limitations in scale, genre diversity, and expert annotation, despite their contributions to specific methodologies [20], [33], [34]. PMEmo, synchronising electrodermal activity signals from 457 subjects with 794 annotated chorus excerpts to compare subjective and autonomic responses, restricts itself to Chinese pop music, and EMOPIA similarly focuses exclusively on pop piano, limiting broader applicability. Notwithstanding these contributions, Table I summarises the characteristics of representative MER datasets and underscores a critical gap: the absence of a large-scale, expert-annotated dataset of pure instrumental music encompassing diverse genres with rigorous inter-annotator reliability protocols. This work addresses this deficiency through the Memo2496 dataset, comprising 2,496 instrumental pieces annotated by 30 certified music specialists proficient in music theory, providing a high-fidelity resource for training robust, generalisable MER systems.

B. Music Emotion Recognition Methods

Traditional MER relies on feature-engineered pipelines. Support Vector Machines classify emotions, whilst Support Vector Regression predicts continuous dimensions such as valence. These methods typically process aggregated acoustic descriptors, including Mel-frequency cepstral coefficients and chroma features. Researchers, such as Kim et al. [37],

TABLE I: Comparisons of Popular Music Emotion Datasets and Memo2496

Dataset	Quantitative (songs)	Data	Raw Data	Annotators
1000songs [31]	1000	Valence, Arousal	✓	crowd-sourcing
AMG1608 [32]	1608	valence, arousal	✗	crowd-sourcing
VGMIDI [33]	200 MIDI pieces	valence	✓	crowd-sourcing
EMOPIA [17]	387 (1087 clips)	Russell's 4Q	✓	piano covers
TROMPA-MER [34]	1161	Valence, Arousal	Downloadable	Public
PMEmo [20]	794	Valence, Arousal and EDA	✓	crowd-sourcing
Memo2496	2496	Valence, Arousal	✓	Certified Musical Specialist

integrate chroma features with statistical classifiers to mitigate timbre-only limitations in valence prediction. Additionally, Lin and Liu [38] demonstrate that two-level SVM classification, informed by genre and prior feature description, mitigates sensitivity to recording conditions, addressing cross-dataset robustness. Deep learning overcomes manual feature design. Convolutional Neural Networks [39] learn time-frequency patterns directly from spectrograms. Long Short-Term Memory networks capture long-term temporal dependencies, alleviating the gradient vanishing problem; these were introduced by Graves et al. [40]. Choi et al. [41] developed Convolutional Recurrent Neural Networks, integrating CNNs' local pattern extraction with RNNs' temporal modelling to account for both spatial and sequential emotion dynamics. More recently, Transformer architectures with self-attention model global contextual relations in MER, circumventing fixed receptive field limitations. Whilst offering flexible feature fusion and enhanced expressiveness, deep learning models still contend with data efficiency, label subjectivity, and limited interpretability in clinical deployment scenarios.

Research in musical emotion recognition MER enhances generalisation via domain adaptation and multimodal fusion. Amjad et al. [42] apply Unsupervised Domain Adaptation UDA to MER with pseudo-label optimisation for annotation noise mitigation. Multimodal fusion includes Quilingking et al.'s [43] late fusion of audio and lyric features for computational efficiency; Zhao and Yoshii's [44] self-attentive architectures integrating symbolic and acoustic features for interpretability via music psychology; and Chen and Li's [45] stacked ensemble learning for heterogeneous feature fusion, improving classification on large datasets. However, current UDA and multimodal architectures assume reliable labels and stationary style distributions. Their deficiency in addressing annotation noise or style drift causes negative transfer and degraded robustness in deployment [46]. Therefore, dual-view and style-aware adaptive MER frameworks are essential, explicitly modelling label reliability and distributional shifts across modalities and datasets.

III. MEMO2496 DATASET

A. Data Collection

The Memo2496 dataset comprises 2496 instrumental music tracks from the Free Music Archive and other reputable online

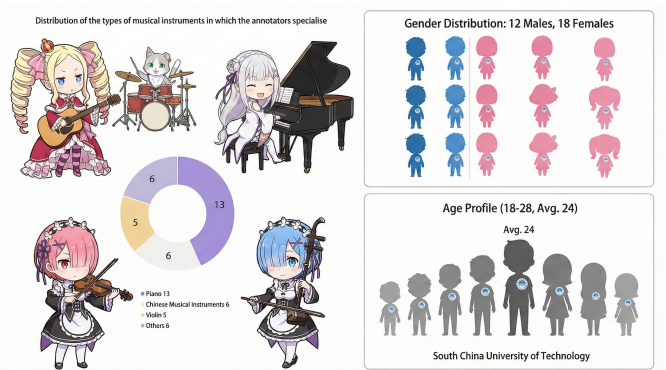


Fig. 1: The distribution of the types of musical instruments in which the annotators specialise

platforms, all Creative Commons Zero (CC0) licensed for unrestricted academic use. This instrumental focus isolates purely acoustic and musical attributes for emotion recognition, eliminating linguistic confounding variables. Preprocessing involves transcoding all tracks to a uniform 44.1 kHz, 16-bit, stereo, 1411 kbps format. Vocal content is then screened using the Spleeter source separation library, which decomposes audio into components including vocals, piano, drums, and bass; tracks exceeding a predetermined vocal energy threshold are excluded. Loudness is subsequently measured and normalised to -23 LUFS in Loudness Units Full Scale, adhering to the EBU R128 standard. Finally, duration filtering removes tracks shorter than 30 seconds or longer than 300 seconds, yielding a curated collection for controlled emotion annotation experiments.

The annotation involved 30 music specialists affiliated with **South China University of Technology**. The team comprised 12 males and 18 females aged 18 to 28 years, with a mean age of 24 years. All annotators possess formal training in music theory and proficiency in at least one musical instrument, suggesting high musical literacy and mitigating potential cognitive barriers. Prior screening confirm the absence of music-related cognitive disorders. Their demographic composition appears in Fig. 1. Annotator backgrounds are diverse across musical specialisations, covering piano, traditional Chinese instruments, violin, and other instruments. This variety benefits MER dataset construction by considering diverse acoustic

properties: percussive attacks, sustained tones, and timbral complexity, informing holistic emotional interpretations. Utilising formally trained specialists, unlike crowdsourced methods, offers anticipated advantages including enhanced inter-annotator agreement, reduced annotation noise, and greater sensitivity to nuances in musical parameters like harmonic progressions, dynamic variations, and musical form. This methodology aims to improve dataset quality for affective computing research.

B. Annotation Protocol

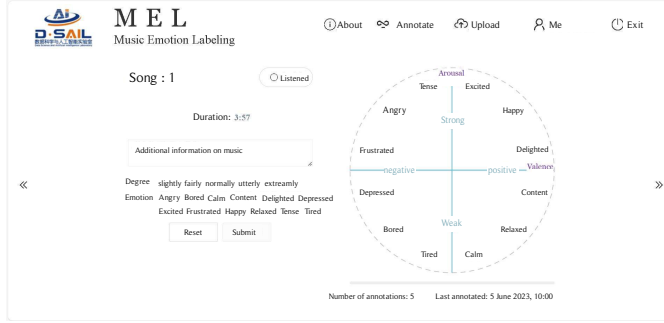


Fig. 2: The interface of annotation is depicted.

The emotion annotation procedure uses a circular (V-A) spatial interface as Fig. 2. The protocol presents 12 discrete emotion terms positioned at theoretical V-A coordinates based on psychological models, with a brief description in Fig. 3. Annotators assign continuous, trajectory-based V-A coordinates to musical excerpts, dynamically adjusting for temporal emotional fluctuations. Intensity is quantified by Euclidean distance from the origin; real-time tracking with emotion anchors enhances labelling precision. A rigorous calibration protocol ensures data quality: annotators train on extreme emotional states and then evaluate 20 tracks, including a covert duplicate for intra-annotator consistency. Calibration requires the mean Euclidean distance between duplicate V-A coordinates not to exceed 0.25, as shown in Fig. 3. This threshold balances stringency and practicality; failing annotators receive retraining, reducing label noise for supervised learning. Annotation accuracy is maintained by a structured rest protocol, including a 15-second cognitive reset interval following each track, mitigating carryover effects. It is crucial to note that the annotations are based on the perceived emotions conveyed by the music, rather than the annotators' personal emotional responses [47], [48]. Daily sessions are capped at one hour. The 2496 tracks are divided into three groups and 30 annotators into three cohorts. A cross-annotation strategy assigns each track group to two distinct cohorts, ensuring each annotator labels 1664 tracks. This distributes workload and enables inter-annotator agreement assessment.

C. Feature Extraction

Mel spectrograms are extracted by first pre-emphasis filtering the raw waveform $x(n)$ defined by $x'(n) = x(n) - 0.97x(n - 1)$. The filtered signal is segmented into N -length

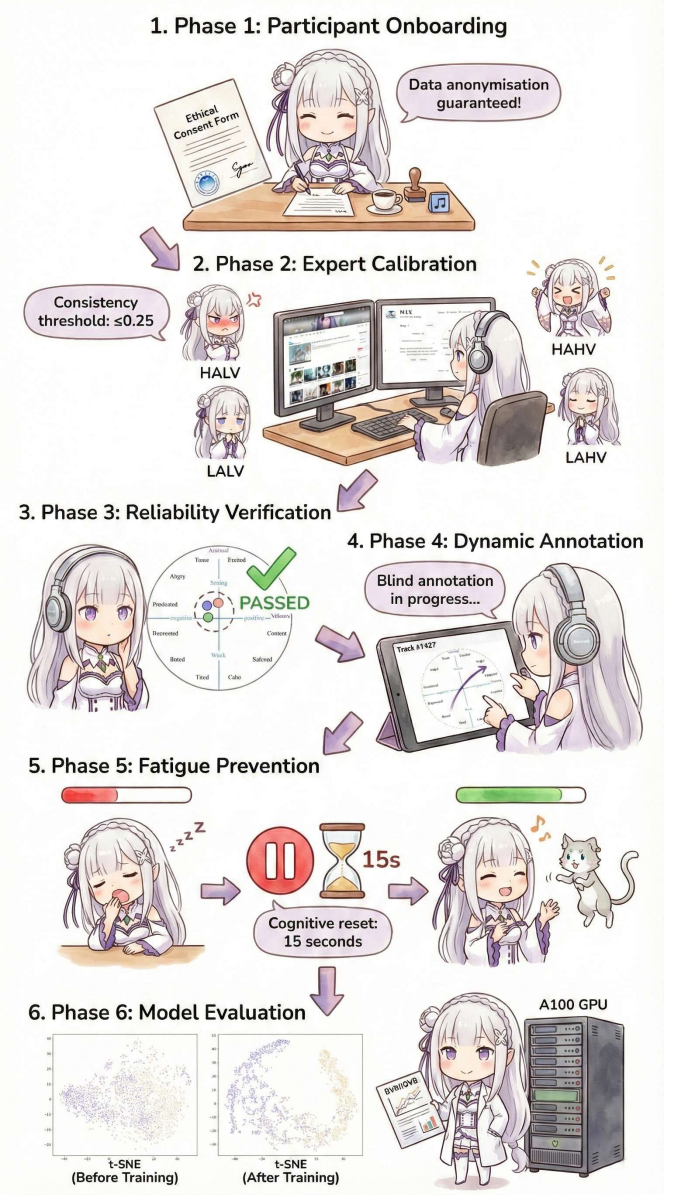


Fig. 3: The Protocol for the annotation experiment is presented.

frames, windowed by a Hamming window, with a 50% overlap ($N/2$ hop length). Each frame undergoes short-time Fourier transform (STFT) computation using a $2N$ -point fast Fourier transform (FFT) for spectral resolution. The magnitude spectrum is subsequently processed by a 128-filter Mel scale bank. Finally, the energy within each Mel band is determined by summing squared magnitudes, followed by natural logarithmic compression. The resultant Mel spectrogram represents time and 128 Mel frequency bands in two dimensions.

Cochleograms model the auditory periphery's frequency analysis. Their extraction involves four steps: applying pre-emphasis and framing consistent with Mel spectrograms; employing an 84-filter Gammatone bank with logarithmically spaced centre frequencies, where each filter models a cochlear filter's impulse response; simulating outer hair cells' nonlinear compression via a power-law function; and finally, \log_{10} trans-

forming the compressed outputs. The resulting cochleograms have dimensions $[N, 84, 87]$. Logarithmic frequency spacing provides enhanced resolution in perceptually significant regions compared to linear spacing. A 60-second segment from 15 to 75 seconds after track onset is processed. This temporal window addresses initial orientation time, mitigates potential onset/offset effects, and reduces fatigue-related annotation degradation, while capturing emotional dynamics.

IV. METHOD IMPLEMENT

A. Overview

The Dual view Adaptive Music Emotion Recogniser DAMER addresses suboptimal heterogeneous acoustic representation fusion, unreliable pseudo label generation, and feature drift across diverse musical styles. Fig. 4 depicts the architecture, which processes Mel spectrograms and cochleograms as two acoustic inputs. Dual Stream Attention Fusion DSAF facilitates token-level bidirectional modality interaction via cross attention. Progressive Confidence Labelling PCL generates high-quality pseudo labels through curriculum-based temperature scaling and two branch consistency. Style Anchored Memory Learning SAML mitigates across-track feature drift using a contrastive memory queue. Three parallel classification heads provide emotion predictions from Mel, cochleogram, and fused representations, supporting standalone or ensemble inference. The modular design allows independent component ablation for assessing individual contributions. The training objective integrates supervised classification, pseudo-label learning, cross-view consistency regularisation, and style-anchored contrastive regularisation.

B. Dual-Stream Attention Fusion (DSAF)

The initial stage of ‘DSAF’ transforms raw time-frequency representations into a unified embedding space suitable for attention-based processing. For the Mel spectrogram, each of the N_{Mel} nodes is linearly projected to a D -dimensional vector:

$$\mathbf{h}_i^{\text{Mel}} = \mathbf{W}_{\text{Mel}} \mathbf{x}_i^{\text{Mel}} + \mathbf{b}_{\text{Mel}}. \quad (1)$$

As in Eqn.1, \mathbf{W}_{Mel} denotes the learnable projection matrix, \mathbf{b}_{Mel} is the bias vector, and $\mathbf{x}_i^{\text{Mel}}$ represents the feature vector of the i -th Mel node. Similarly, cochleogram nodes undergo projection:

$$\mathbf{h}_j^{\text{Coch}} = \mathbf{W}_{\text{Coch}} \mathbf{x}_j^{\text{Coch}} + \mathbf{b}_{\text{Coch}} \quad (2)$$

In Eqn.2, \mathbf{W}_{Coch} and \mathbf{b}_{Coch} are the corresponding cochleogram projection parameters. The resulting token sequences are denoted $\mathbf{H}^{\text{Mel}} \in \mathbb{R}^{B \times N_{\text{Mel}} \times D}$ and $\mathbf{H}^{\text{Coch}} \in \mathbb{R}^{B \times N_{\text{Coch}} \times D}$, where B represents the batch size and D is the embedding dimension. This tokenisation strategy treats each time-frequency bin as an independent semantic unit, thereby enabling fine-grained cross-modal interaction in subsequent attention layers.

The core innovation of ‘DSAF’ lies in its bidirectional cross-attention architecture, where each acoustic view attends to the complementary representation. For Mel tokens querying cochleogram context, the multi-head attention operation is formulated in Eqn.3:

$$\mathbf{H}_{\text{Mel} \leftarrow \text{Coch}} = \text{MHA}(\mathbf{Q} = \mathbf{H}^{\text{Mel}}, \mathbf{K} = \mathbf{H}^{\text{Coch}}, \mathbf{V} = \mathbf{H}^{\text{Coch}}). \quad (3)$$

Here, MHA denotes multi-head attention with H heads. Symmetrically, cochleogram tokens attend to Mel representations:

$$\mathbf{H}_{\text{Coch} \leftarrow \text{Mel}} = \text{MHA}(\mathbf{Q} = \mathbf{H}^{\text{Coch}}, \mathbf{K} = \mathbf{H}^{\text{Mel}}, \mathbf{V} = \mathbf{H}^{\text{Mel}}). \quad (4)$$

Each attention head computes scaled dot-product attention independently as Eqn.4. For head h , the attention weights are:

$$\text{Attention}(\mathbf{Q}, \mathbf{K}, \mathbf{V}) = \text{softmax} \left(\frac{\mathbf{Q}\mathbf{K}^T}{\sqrt{d_k}} \right) \mathbf{V}. \quad (5)$$

In Eqn.5, d_k is the dimension per head. Following standard Transformer conventions, residual connections and Layer Normalisation are applied.

$$\mathbf{H}' = \text{LN}(\mathbf{H} + \text{Dropout}(\text{MHA}(\mathbf{Q}, \mathbf{K}, \mathbf{V}), p_{\text{dropout}})), \quad (6)$$

$$\mathbf{H}'' = \text{LN}(\mathbf{H}' + \text{Dropout}(\text{FFN}(\mathbf{H}'), p_{\text{dropout}})). \quad (7)$$

In these equations, LN denotes Layer Normalisation, and Dropout regularisation is applied with probability p_{dropout} . Subsequently, a position-wise Feed-Forward Network (FFN) with GELU activation further refines the representations.

$$\text{FFN}(\mathbf{x}) = \text{Linear}_2(\text{GELU}(\text{Linear}_1(\mathbf{x}))). \quad (8)$$

The ‘FFN’ in Eqn.8 employs two linear transformations, Linear_1 and Linear_2 , which implement expansion and contraction of dimensions with a factor of 4. The complete cross-view layer is stacked L times, enabling progressive refinement of cross-modal dependencies.

C. Progressive Confidence Labelling (PCL)

Pseudo-label generation in semi-supervised learning is susceptible to confirmation bias, where erroneous early predictions are reinforced through iterative training. To mitigate this, ‘PCL’ implements a curriculum-based temperature scheduling strategy that modulates prediction sharpness across training epochs. The temperature parameter τ_t at epoch t is defined in Eqn.9:

$$\tau_t = \tau_{\text{max}} - (\tau_{\text{max}} - \tau_{\text{min}}) \frac{t}{T_{\text{total}}}. \quad (9)$$

Here, t denotes the current epoch, T_{total} is the total number of epochs, $\tau_{\text{min}} = 0.7$ is the minimum temperature bound, and $\tau_{\text{max}} = 1.5$ is the maximum temperature bound. In early training stages ($t \ll T_{\text{total}}$), elevated temperatures ($\tau_t \approx \tau_{\text{max}}$) yield softened probability distributions, preventing premature commitment to potentially incorrect predictions. As training progresses ($t \rightarrow T_{\text{total}}$), reduced temperatures ($\tau_t \rightarrow \tau_{\text{min}}$) sharpen distributions, enabling confident pseudo-label assignment.

Temperature τ_t descends from 1.50 to 0.70, progressively sharpening probability distributions to enhance prediction confidence. As training progresses, where $t \rightarrow T_{\text{total}}$, reduced temperatures sharpen distributions, enabling confident pseudo-label assignment. Temperature-scaled softmax probabilities for the two branches are computed as:

$$\mathbf{p}^{\text{Mel}} = \text{softmax}(\mathbf{z}^{\text{Mel}} / \tau_t), \quad (10)$$

$$\mathbf{p}^{\text{Coch}} = \text{softmax}(\mathbf{z}^{\text{Coch}} / \tau_t). \quad (11)$$

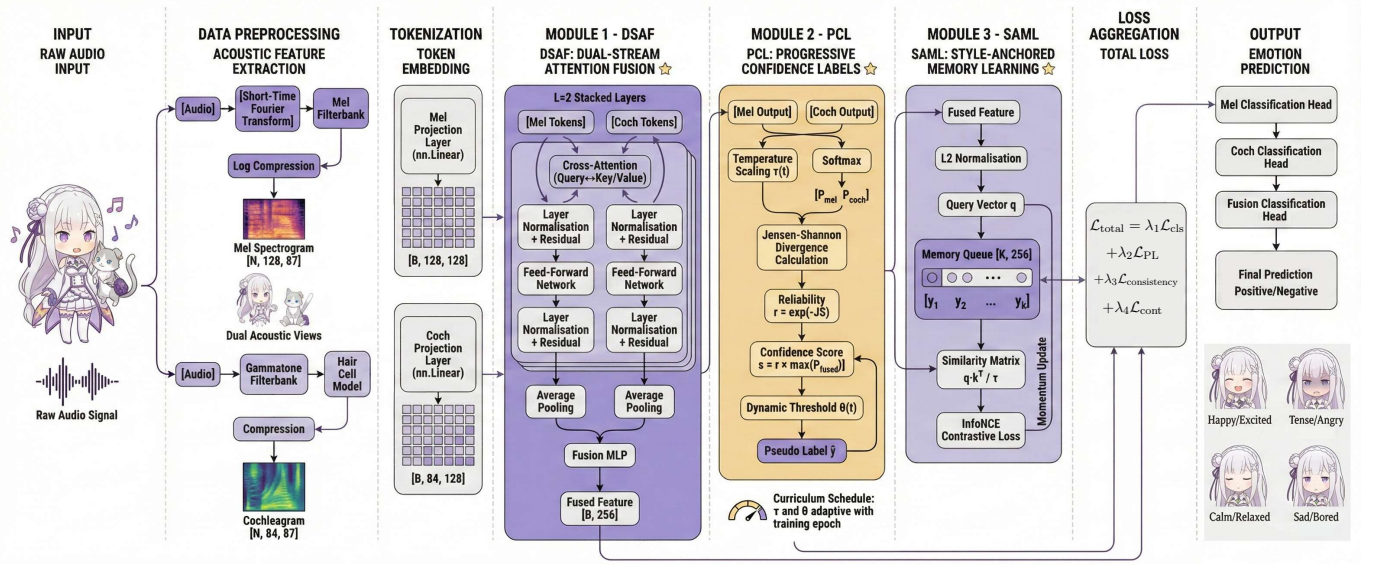


Fig. 4: The DAMER framework is illustrated.

This annealing schedule aligns with curriculum learning principles, where model capacity is progressively allocated to increasingly challenging discrimination tasks.

The reliability of pseudo-labels is assessed through cross-view prediction consistency. The Jensen-Shannon (JS) divergence quantifies the discrepancy between Mel and cochleagram probability distributions:

$$JS(p^{Mel}, p^{Coch}) = \frac{1}{2}KL(p^{Mel}||M) + \frac{1}{2}KL(p^{Coch}||M) \quad (12)$$

In Eqn.12, $M = \frac{1}{2}(p^{Mel} + p^{Coch})$ is the mixture distribution, and KL denotes the Kullback-Leibler divergence. The JS divergence is bounded within $[0, \log 2]$, with lower values indicating greater inter-view agreement. A reliability score r is derived through exponential transformation:

$$r = \exp(-JS(p^{Mel}, p^{Coch})). \quad (13)$$

Eqn.13 yields $r \in [e^{-\log 2}, 1] \approx [0.5, 1]$, where values approaching unity indicate high cross-view consistency. The fused probability distribution is computed as:

$$p^{Fuse} = \frac{1}{2}(p^{Mel} + p^{Coch}). \quad (14)$$

The composite confidence score c integrates reliability with prediction certainty:

$$c = r \cdot \max(p^{Fuse}). \quad (15)$$

As Eqn.15, $\max(p^{Fuse})$ represents the maximum class probability in the fused distribution. This mechanism constitutes the dual-branch consistency, which is later used for regularisation.

To progressively incorporate unlabelled samples as training stabilises, a dynamic threshold θ_t governs pseudo-label selection:

$$\theta_t = \theta_0 - (\theta_0 - \theta_{min}) \frac{t}{T_{total}}. \quad (16)$$

In Eqn.16, θ_0 is the initial threshold, for example $\theta_0 = 0.9$, and θ_{min} establishes the lower bound, for instance $\theta_{min} = 0.7$.

Samples satisfying $c \geq \theta_t$ are assigned pseudo-labels. Let \mathcal{D}_{PL} denote this subset of pseudo-labelled samples. The pseudo-label loss \mathcal{L}_{PL} is computed as reliability-weighted cross-entropy over \mathcal{D}_{PL} :

$$\mathcal{L}_{PL} = \frac{1}{|\mathcal{D}_{PL}|} \sum_{(\mathbf{x}, y_{PL}) \in \mathcal{D}_{PL}} r \cdot CE(\mathbf{y}, y_{PL}), \quad (17)$$

CE denotes cross-entropy loss, and y_{PL} are the assigned pseudo-labels. The reliability weighting ensures that samples with higher dual-branch agreement exert greater influence on parameter updates, thereby reducing the propagation of noisy pseudo-labels.

D. Style-Anchored Memory Learning (SAML)

Musical emotion recognition is complicated by substantial stylistic heterogeneity across-tracks, leading to feature drift that degrades classifier generalisation. ‘SAML’ addresses this challenge by maintaining a sliding memory queue \mathcal{Q} that stores the most recent fusion features and their corresponding labels. The queue is updated via enqueue-dequeue operations after each mini-batch:

$$Q[P_Q] = \text{L2-Normalise}(p^{Fuse}). \quad (18)$$

In Eqn.18, P_Q is a circular pointer incremented modulo the queue size, specifying the position for the incoming batch of ‘L2’-normalised fused features. This update strategy ensures a smooth queue evolution by continuously replacing the oldest features with the newest ones, effectively providing a moving average of feature distributions. This prevents abrupt distributional shifts that could destabilise contrastive learning dynamics.

‘SAML’ employs an ‘InfoNCE’-style supervised contrastive objective that encourages clustering of same-class samples while repelling different-class instances. For a normalised

query feature \mathbf{q} with label y_q , the contrastive loss is defined in Eqn.19:

$$\mathcal{L}_{\text{cont}}(\mathbf{q}, y_q) = - \sum_{j=1}^{|\mathcal{Q}|} \mathbb{I}(y_q = y_j) \log \frac{\exp(\mathbf{q} \cdot \mathbf{k}_j / \tau_{\text{cont}})}{\sum_{k=1}^{|\mathcal{Q}|} \exp(\mathbf{q} \cdot \mathbf{k}_k / \tau_{\text{cont}})}. \quad (19)$$

Here, τ_{cont} is the contrastive temperature, for example $\tau_{\text{cont}} = 0.07$. \mathbf{k}_j denotes the j -th key in the memory queue, and $\mathbb{I}(\cdot)$ is the indicator function. The batch-averaged contrastive loss for a batch of N_q queries is:

$$\mathcal{L}_{\text{cont}} = \frac{1}{N_q} \sum_{i=1}^{N_q} \mathcal{L}_{\text{cont}}(\mathbf{q}_i, y_{q_i}). \quad (20)$$

By anchoring Eqn.20 to historical same-class exemplars distributed across diverse tracks and styles, ‘SAML’ enforces emotion-discriminative feature invariance, thereby suppressing style-specific confounders.

E. Training Objective and Optimisation

The complete training objective integrates supervised classification, pseudo-label learning, cross-view consistency regularisation, and style-anchored contrastive regularisation. The training process of DAMER is depicted in Algorithm 1. The total loss $\mathcal{L}_{\text{total}}$ is defined:

$$\mathcal{L}_{\text{total}} = \lambda_1 \mathcal{L}_{\text{cls}} + \lambda_2 \mathcal{L}_{\text{PL}} + \lambda_3 \mathcal{L}_{\text{consistency}} + \lambda_4 \mathcal{L}_{\text{cont}}. \quad (21)$$

The classification loss \mathcal{L}_{cls} comprises cross-entropy for the Mel-branch, cochleagram-branch, and fusion-branch predictions:

$$\mathcal{L}_{\text{cls}} = \text{CE}(\mathbf{z}^{\text{Mel}}, y) + \text{CE}(\mathbf{z}^{\text{Coch}}, y) + \text{CE}(\mathbf{z}^{\text{Fuse}}, y). \quad (22)$$

In Eqn.22, y represents the ground-truth labels. The consistency regularisation $\mathcal{L}_{\text{consistency}}$ encourages alignment between branch-specific representations by minimising the Jensen-Shannon divergence between their probability distributions:

$$\mathcal{L}_{\text{consistency}} = \text{JS}(\mathbf{p}^{\text{Mel}}, \mathbf{p}^{\text{Coch}}) \quad (23)$$

Default loss weights in Eqn.21 are set as $\lambda_1 = 1.0$, $\lambda_2 = 0.8$, $\lambda_3 = 0.2$, and $\lambda_4 = 0.1$. These values are determined through grid search on the validation set. This multi-objective formulation balances discriminative learning with regularisation constraints, enabling robust generalisation across heterogeneous musical corpora.

V. EXPERIMENTS AND ANALYSIS

A. Experimental Implementation

Experiments are conducted on three publicly available MER datasets: Memo2496, 1000songs, and PMEMo. For all datasets, a stratified 70%/30% train/test split is employed to ensure balanced class distributions across partitions. Both Arousal and Valence dimensions are evaluated independently as binary classification tasks, with labels binarised at the zero threshold.

The DAMER architecture is configured with embedding dimension $D = 128$, fusion dimension $D_f = 256$, $H = 4$ attention heads, and $L = 2$ cross-view transformer layers.

Algorithm 1 DAMER Training Procedure

Require: Mel spectrograms $\mathbf{X}^{(m)}$, Cochleograms $\mathbf{X}^{(c)}$, Labels \mathbf{y} , Epochs T

Ensure: Trained model parameters Θ

- 1: Initialise model, memory queue Q , pointer $p \leftarrow 0$
- 2: **for** $t = 1$ to T **do**
- 3: $\rho \leftarrow (t-1)/T$
- 4: $\tau \leftarrow \tau_{\text{min}} + (1-\rho)(\tau_{\text{max}} - \tau_{\text{min}})$
- 5: $\theta \leftarrow \max(\theta_{\text{min}}, \theta_0 \cdot (1-\rho))$
- 6: **for** each batch $(\mathbf{x}^{(m)}, \mathbf{x}^{(c)}, \mathbf{y})$ **do**
- 7: $\mathbf{H}^{(m)} \leftarrow \text{MelProjection}(\mathbf{x}^{(m)}); \mathbf{H}^{(c)} \leftarrow \text{CochProjection}(\mathbf{x}^{(c)})$
- 8: **for** $l = 1$ to L **do**
- 9: $\mathbf{H}^{(m)}, \mathbf{H}^{(c)} \leftarrow \text{CrossViewLayer}(\mathbf{H}^{(m)}, \mathbf{H}^{(c)})$
- 10: $\mathbf{z}^{(m)} \leftarrow \text{AvgPool}(\mathbf{H}^{(m)}); \mathbf{z}^{(c)} \leftarrow \text{AvgPool}(\mathbf{H}^{(c)})$
- 11: $\mathbf{z}^{(f)} \leftarrow \text{FusionMLP}([\mathbf{z}^{(m)} \parallel \mathbf{z}^{(c)}])$
- 12: $\mathbf{o}^{(m)}, \mathbf{o}^{(c)}, \mathbf{o}^{(f)} \leftarrow \text{ClassifierHeads}(\mathbf{z}^{(m)}, \mathbf{z}^{(c)}, \mathbf{z}^{(f)})$
- 13: $\mathbf{P}^{(m)} \leftarrow \text{softmax}(\mathbf{o}^{(m)} / \tau); \mathbf{P}^{(c)} \leftarrow \text{softmax}(\mathbf{o}^{(c)} / \tau)$
- 14: $r \leftarrow \exp(-\text{JS}(\mathbf{P}^{(m)}, \mathbf{P}^{(c)})); s \leftarrow r \cdot \max(\mathbf{P}^{(f)})$
- 15: Select $\mathcal{S} \leftarrow \{i : s_i \geq \theta\}$; assign $\hat{\mathbf{y}} \leftarrow \arg \max(\mathbf{P}^{(f)})$
- 16: $\mathcal{L} \leftarrow \mathcal{L}_{\text{cls}} + \mathcal{L}_{\text{PL}}(\mathcal{S}, r) + \mathcal{L}_{\text{consistency}} + \mathcal{L}_{\text{cont}}$
- 17: Backpropagate(\mathcal{L}); UpdateParameters(Θ)
- 18: UpdateMemoryQueue($Q, \mathbf{z}^{(f)}, \mathbf{y}, p$)

The memory queue size is set to $K = 512$ with momentum coefficient 0.95. For instance, $\tau_{\text{min}} = 0.7$ and $\tau_{\text{max}} = 1.5$, whilst dynamic threshold parameters are $\theta_0 = 0.65$ and $\theta_{\text{min}} = 0.35$. Loss weights are configured as $\lambda_1 = 1.0$, $\lambda_2 = 0.8$, $\lambda_3 = 0.2$, and $\lambda_4 = 0.1$. The model is optimised using Adam with an initial learning rate of 1×10^{-3} and weight decay of 1×10^{-4} , trained for 80 epochs with cosine annealing learning rate scheduling. Mixed-precision training with gradient clipping (maximum norm 5.0) is employed for computational efficiency. The dataset is accessible from Figshare: doi.org/10.6084/m9.figshare.25827034 and data.cs.scut.edu.cn, with a detailed description, tutorial of the dataset usage and code of DAMER. All experiments are conducted on an NVIDIA A100 80GB GPU using PyTorch 1.13.0 with CUDA 12.1. Performance is evaluated using Accuracy (ACC), F1-score, and Area Under the ROC Curve (AUC).

B. Experiments on MER Datasets

Comprehensive comparisons are conducted against twelve baseline methods spanning traditional machine learning approaches, deep learning architectures, and recent MER-specific models. Traditional baselines include Support Vector Machines (SVM) [49] with handcrafted acoustic features. Deep learning baselines encompass Residual GCB-net [50], which employs graph convolutional networks for music feature learning, and UDDA [46], which applies unsupervised domain adaptation with pseudo-label optimisation. Recent state-of-the-art methods include MOCNN [51] for multi-scale convolutional feature extraction, ATDGNN [52] for attention-based

TABLE II: Comparisons of the Mean Accuracies (ACC) / F1 score / AUC score of Music Emotion Recognition on Memo2496

Model	Arousal			Valence		
	Acc	F1	AUC	Acc	F1	AUC
SVM* [49]	66.83	58.34	65.96	70.48	79.64	59.69
RGCB-net* [50]	77.11	69.42	76.37	76.72	84.96	61.50
UDDA† [46]	77.74	74.96	85.37	77.55	77.72	65.41
MOCNN† [51]	77.24	72.37	77.94	76.91	85.94	67.75
ATDGNN† [52]	73.89	74.10	84.73	76.87	84.97	75.46
mADCRNN† [53]	78.78	73.64	86.25	77.71	70.08	84.39
DSTFN† [54]	78.04	72.41	85.91	78.21	86.24	75.34
IIOF [55]	78.14	73.28	85.33	78.36	86.44	76.81
ADFF [56]	75.55	72.77	86.03	78.19	86.89	76.91
EmotionIC [56]	76.56	72.13	85.60	77.45	85.85	74.53
SECapEmotion [57]	78.21	71.54	84.32	78.21	78.74	71.54
MCGC-net [58]	79.52	72.44	78.09	78.61	87.07	68.29
DAMER	82.95	80.70	90.21	78.34	84.72	83.31

*: official code under identical settings; †: the re-implementation; unmarked values are quoted from original papers.

TABLE III: Comparisons of the Mean Accuracies (ACC) / F1 score / AUC score of Music Emotion Recognition on 1000songs

Model	Arousal			Valence		
	Acc	F1	AUC	Acc	F1	AUC
SVM* [49]	59.85	64.89	60.82	53.39	53.41	58.77
RGCB-net* [50]	78.66	83.82	77.56	68.71	77.68	64.15
UDDA† [46]	77.97	76.45	78.13	68.93	79.42	66.59
MOCNN† [51]	77.64	82.25	77.99	68.24	69.51	64.56
ATDGNN† [52]	77.72	80.87	77.02	68.17	74.35	72.23
mADCRNN† [53]	77.97	80.99	78.07	65.93	75.12	72.12
DSTFN† [54]	78.94	84.58	77.69	68.71	76.95	71.40
IIOF [55]	77.03	85.24	78.82	69.91	79.77	73.70
ADFF [56]	77.31	85.03	78.79	68.32	75.22	73.12
EmotionIC [56]	67.63	74.79	71.38	69.42	79.32	71.78
SECapEmotion [57]	78.50	83.19	85.70	69.67	78.74	71.54
MCGC-net [58]	79.03	84.49	78.21	70.05	79.42	66.59
DAMER	81.28	82.32	89.15	70.74	72.79	77.28

TABLE IV: Comparisons of the Mean Accuracies (ACC) / F1 score / AUC score of Music Emotion Recognition on PMEMo

Model	Arousal			Valence		
	Acc	F1	AUC	Acc	F1	AUC
SVM* [49]	49.06	59.42	53.11	53.93	64.83	50.91
RGCB-net* [50]	84.76	90.60	72.33	74.32	84.86	64.21
UDDA† [46]	82.83	89.06	73.19	75.91	81.57	67.19
MOCNN† [51]	84.69	90.45	74.72	75.18	84.38	64.77
ATDGNN† [52]	83.50	90.94	85.08	74.83	85.12	77.21
mADCRNN† [53]	84.80	90.47	83.11	74.94	85.28	78.36
DSTFN† [54]	83.74	90.33	83.63	75.91	85.34	76.84
IIOF [55]	84.49	91.96	84.44	75.66	85.41	76.83
ADFF [56]	83.76	90.81	84.97	73.74	84.88	78.02
EmotionIC [56]	84.37	90.79	84.06	74.03	84.86	74.44
SECapEmotion [57]	82.38	90.16	80.45	75.56	85.26	76.20
MCGC-net [58]	85.81	91.42	75.12	75.42	85.11	69.81
DAMER	85.98	90.58	74.33	77.61	85.54	79.71

temporal-domain graph neural networks, mADCRNN [53] for hybrid attention-dilated convolutional recurrent networks, DSTFN [54] for dual-stream temporal fusion networks, IIOF [55] for inter-intra object fusion, ADFF [56] for attention-driven feature fusion, EmotionIC [56] for emotion-informed classification, SECapEmotion [57] for self-enhanced capsule networks, and MCGC-net [58] for multi-scale controllable graph convolutional networks. Methods marked with asterisks utilise official implementations under identical settings, whilst those marked with daggers are re-implemented following original specifications; unmarked results are quoted from original publications.

As presented in Table II, DAMER achieves state-of-the-art performance on Memo2496, attaining 82.95% accuracy, 80.70% F1-score, and 90.21% AUC on the Arousal dimension, representing improvements of 3.43%, 8.26%, and 3.96% over the strongest baseline (MCGC-net), respectively. On the Valence dimension, DAMER achieves competitive performance with 78.34% accuracy and 83.31% AUC. Table III demonstrates consistent improvements on 1000songs, where DAMER obtains 81.28% accuracy and 89.15% AUC for Arousal, and 70.74% accuracy with 77.28% AUC for Valence, surpassing all baselines. Table IV shows that on PMEMo, DAMER achieves 85.98% accuracy for Arousal and 77.61% accuracy with 79.71% AUC for Valence, establishing new state-of-the-art results. The consistent performance gains across three diverse datasets with varying annotation methodologies (expert vs. crowdsourced) and musical styles (instrumental vs. pop) validate the generalisation capability of the proposed framework.

TABLE V: The Mean Accuracies (ACC) for Ablation Study on Memo2496, 1000songs and PMEMo

Module			MemoEmo2496		1000songs		PMEmo	
DSAF	PCL	SAML	Arousal	Valence	Arousal	Valence	Arousal	Valence
✓	✓	✓	80.94	77.40	79.02	69.51	84.44	75.50
			80.58	77.34	78.69	69.42	83.01	75.06
✓	✓	✓	78.38	75.79	78.14	68.46	82.95	74.23
			81.89	77.07	80.67	70.34	85.78	77.10
✓	✓	✓	81.61	74.61	81.03	69.49	83.78	76.03
			81.08	75.59	79.36	69.55	84.23	74.09
✓	✓	✓	82.95	78.34	81.28	70.93	85.98	77.61

C. Ablation Study

Systematic ablation experiments quantify the individual contributions of each proposed module, with results presented in Table V for three datasets and both Arousal and Valence dimensions. Among single-module configurations on Memo2496 Arousal, DSAF achieves the highest accuracy with ‘80.94%’, utilising cross-view fusion for acoustic information. PCL alone yields ‘80.58%’ Arousal accuracy, providing meaningful curriculum-based pseudo-labelling supervision. SAML independently attains ‘78.38%’ Arousal accuracy, offering improvements via contrastive memory regularisation to anchor style-invariant features. Pairwise module combinations demonstrate improved performance over single modules on Memo2496 Arousal. For example, DSAF combined with PCL achieves ‘81.89%’ Arousal accuracy, surpassing DSAF alone and benefiting from cross-view fusion enhanced representations. The DSAF plus SAML combination yields ‘81.08%’ accuracy, whilst PCL plus SAML attains ‘81.61%’. The complete DAMER framework, integrating all three modules, achieves the highest observed performance across all datasets and dimensions: ‘82.95%’ Arousal and ‘78.34%’ Valence accuracy on Memo2496; ‘81.28%’ Arousal and ‘70.93%’ Valence on 1000songs; and ‘85.98%’ Arousal and ‘77.61%’ Valence on PMEMo. These results indicate complementary module operation: DSAF provides multi-view representations, PCL offers pseudo-label supervision, and SAML enforces style-invariant features, collectively enabling superior generalisation across heterogeneous musical corpora.

D. Progressive Confidence Labelling Dynamics

Figure 5 illustrates the efficacy of the Progressive Confidence Labelling module, hereafter referred to as PCL, by demonstrating the temporal evolution of curriculum metrics across training epochs. This three-panel visualization reveals that the DAMER curriculum-based pseudo-labelling strategy maintains consistently high prediction quality while progressively refining sample selection criteria.

The top panel depicts the trajectories of confidence and reliability scores. Both metrics, representing their mean values, stabilize near 0.90 throughout training with diminishing standard deviations. This indicates that dual-branch consistency quantification via Jensen-Shannon divergence successfully identifies high-quality pseudo-labels.

The middle panel demonstrates that pseudo-label coverage, defined as the mask ratio, remains above 0.92, while pseudo-label strength, an average pseudo-label probability, sustains

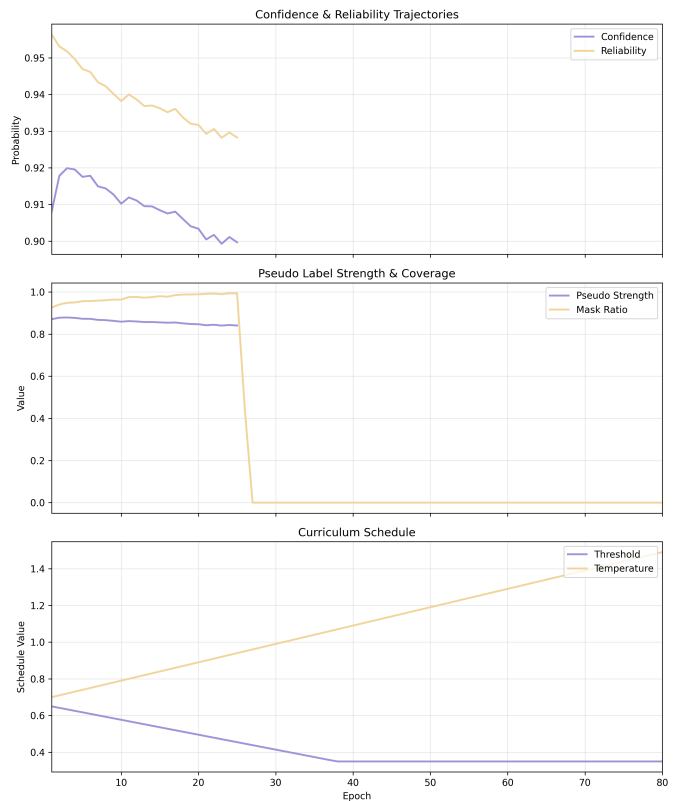


Fig. 5: Progressive Confidence Labelling dynamics across training epochs. Top: confidence and reliability score trajectories stabilising near 0.90. Middle: pseudo-label strength and mask ratio demonstrating sustained coverage above 0.92. Bottom: curriculum schedule showing temperature **descent** from 1.50 to 0.70 and threshold descent from 0.65 to 0.35.

a plateau exceeding 0.87 in later epochs. This validates the strict-to-lenient transition strategy, wherein early-stage high thresholds (starting at 0.65) ensure only high-confidence samples generate pseudo-labels to prevent noise propagation, whilst late-stage low thresholds (descending to 0.35) progressively incorporate more samples as model reliability improves.

The bottom panel exhibits the scheduled annealing of curriculum hyperparameters. Temperature τ_t **descends** from 1.50 to 0.70, progressively **sharpening** probability distributions to enhance prediction confidence. Threshold ‘ θ_t ’ descends from 0.65 to 0.35, enabling gradual incorporation of previously ambiguous samples as cross-view agreement improves. This coordinated scheduling is underpinned by architectural syner-

gies. The Dual-Stream Attention Fusion module, hereafter referred to as DSAF, provides complementary Mel-cochleagram representations that reduce inter-branch divergence, thereby elevating reliability scores ' $r = \exp(-JS)$ '. The Style-Anchored Memory Learning module, hereafter referred to as SAML, suppresses cross-view feature drift through contrastive clustering, which indirectly stabilizes pseudo-label assignment. These dynamics collectively substantiate that PCL effectively balances pseudo-label coverage with quality. This approach avoids instability characteristic of fixed-threshold semi-supervised methods and ensures curriculum adaptation aligns with model capacity evolution rather than arbitrary epoch-based schedules.

E. Style-Anchored Memory Learning Effectiveness

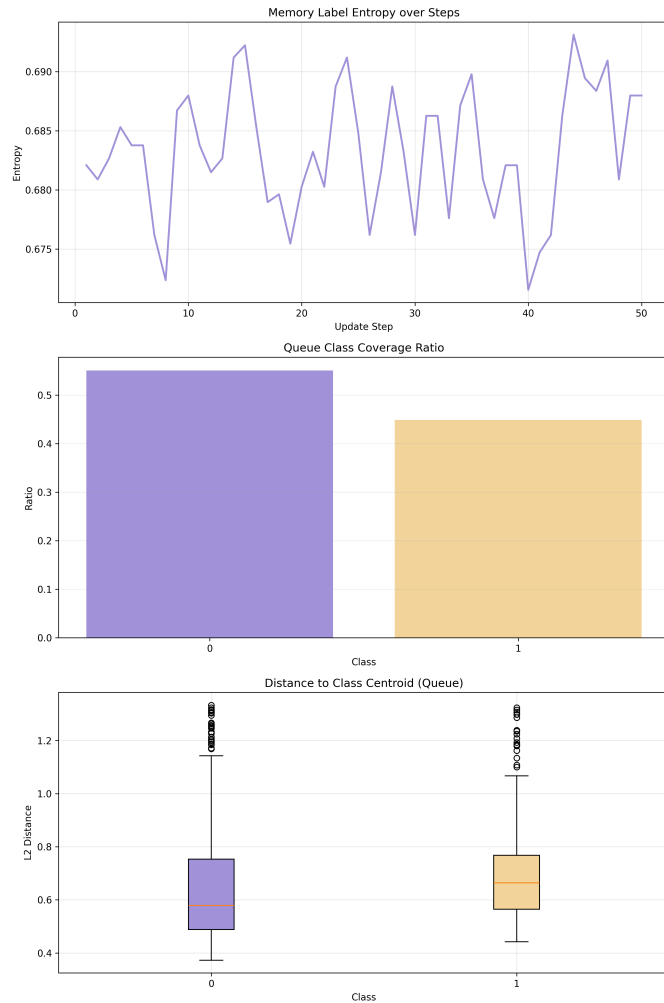


Fig. 6: Style-Anchored Memory Learning effectiveness visualisation. Top: memory label entropy oscillating within a narrow band (0.685 ± 0.007) across update steps. Middle: queue class coverage ratio exhibiting near-balanced distribution (55%:45%). Bottom: L2 distances from samples to class centroids demonstrating compact intra-class clustering.

The Style-Anchored Memory Learning SAML module effectively mitigates cross-track feature drift, as evidenced by

three complementary metrics. The upper panel of Fig. 6 shows memory label entropy oscillating over queue update steps, centred at 0.685 with a standard deviation of 0.007. This suggests the momentum-updated queue maintains stable class representation, preventing single-class dominance or excessive dispersion. The middle panel reveals an approximately balanced 55%/45% split in queue class coverage for Class 0 and Class 1, indicating class balance is maintained for contrastive learning efficacy. The lower panel presents L2 distances from queue samples to their class centroids; both Class 0 and Class 1 exhibit low median distances, approximately 0.60 and 0.65, with compact interquartile ranges, confirming intra-class compactness despite musical style heterogeneity within the Memo2496 corpus. These outcomes align with SAML's architectural design. Stable entropy and balanced coverage are facilitated by a 0.95 momentum coefficient, which promotes gradual queue evolution and prevents abrupt distributional shifts. Simultaneously, supervised InfoNCE loss enforces attraction of same-class samples and repulsion of different-class instances, contributing to intra-class compactness. Beyond these core mechanisms, architectural synergies further enhance SAML performance. The Dual-Stream Attention Fusion DSAF module generates complementary Mel-cochleagram representations, enriching contrastive attributes and supporting stable entropy and coverage. Concurrently, the Progressive Confidence Labelling PCL module supplies high-reliability pseudo-labels, reducing memory queue noise and promoting intra-class compactness. Collectively, the stabilization of entropy, balanced coverage, and tight intra-class clustering indicate SAML effectively anchors emotion-discriminative features to style-invariant representations, supporting cross-corpus generalisation in music emotion recognition.

F. T-SNE Visualisation

The discriminative capacity of learned representations is assessed through t-distributed Stochastic Neighbour Embedding (t-SNE) visualisation of fusion features before and after training, as depicted in Fig. 7. The left panel illustrates the initial feature distribution at epoch 0, where samples from both emotion classes (positive and negative) exhibit substantial overlap and lack discernible clustering structure, reflecting the random initialisation of network parameters and the absence of emotion-discriminative representations.

This visualisation provides interpretable evidence that DAMER successfully learns emotion-discriminative feature representations. The observed clustering behaviour validates the effectiveness of the three proposed modules operating in concert: DSAF enables informative cross-view feature fusion, PCL contributes high-quality pseudo-label supervision that refines class boundaries, and SAML enforces intra-class compactness through contrastive memory anchoring. The clear class separation achieved in the learned embedding space underpins the strong classification performance reported in quantitative evaluations.

VI. CONCLUSION

This paper presents the Dual-view Adaptive Music Emotion Recogniser (DAMER) framework and the Memo2496 dataset

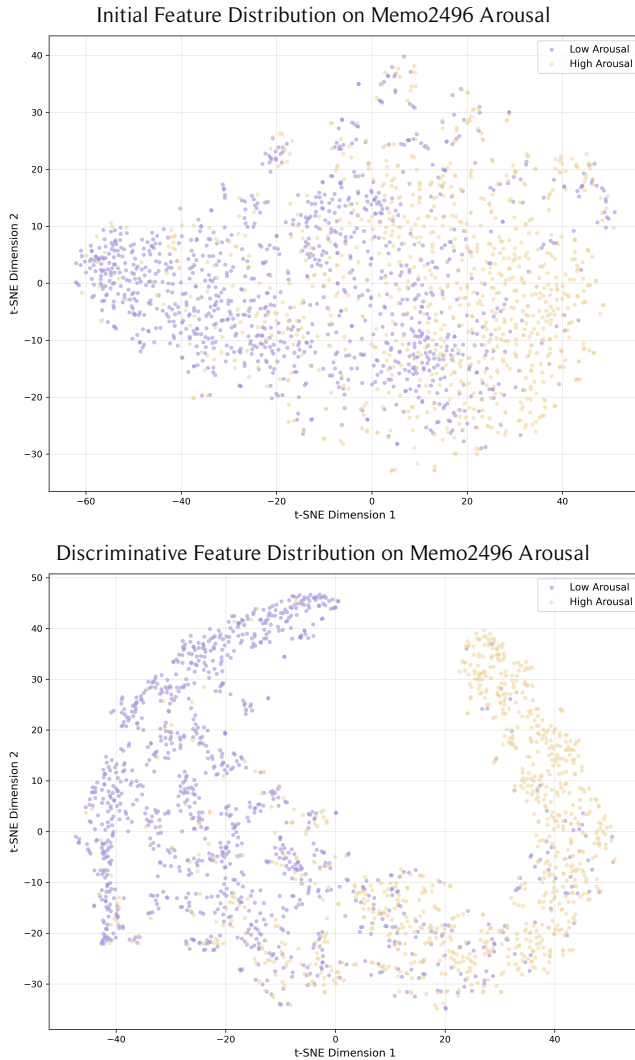


Fig. 7: The T-SNE visualisation method illustrates the changes in feature distribution before and after training.

for music emotion recognition. Memo2496 is one of the largest expert-annotated instrumental music emotion datasets, featuring 2496 tracks with continuous Valence and Arousal labels from 30 specialists. This dataset ensures high reliability and reduced label noise, addressing crowdsourced limitations. DAMER integrates three modules: its Dual-Stream Attention Fusion module leverages complementary acoustic features from Mel spectrograms and cochleograms via bidirectional cross-attention; its Progressive Confidence Labelling module generates reliable pseudo-labels via curriculum-based temperature scheduling and Jensen–Shannon divergence based consistency, mitigating confirmation bias; and its Style-Anchored Memory Learning module maintains a contrastive memory queue, anchoring emotion-discriminative features to style-invariant representations, suppressing cross-track feature drift. Experiments on Memo2496, 1000songs, and PMemo demonstrate DAMER achieves superior performance across Arousal and Valence. Ablation and visualisation analyses provide evidence for its efficacy and generalisation across diverse datasets. The Memo2496 dataset and DAMER source code

are publicly released, facilitating reproducible research.

VII. ACKNOWLEDGMENTS

The author, Qilin Li, extends heartfelt gratitude to Emilia, the central character of the light novel *Re:Life in a Different World from Zero*. Emilia, a half-elf with long silver hair and cyanine eyes residing in the elfin forests of the permafrost, inspires the colour schemes used in the illustrations and provides invaluable spiritual support throughout the author's creative journey.

REFERENCES

- [1] R. Panda, R. Malheiro, and R. P. Paiva, "Audio features for music emotion recognition: A survey," *IEEE Transactions on Affective Computing*, vol. 14, no. 1, pp. 68–88, 2023.
- [2] Y.-H. Yang and H. H. Chen, "Machine recognition of music emotion: A review," *ACM Trans. Intell. Syst. Technol.*, vol. 3, no. 3, May 2012. [Online]. Available: <https://doi.org/10.1145/2168752.2168754>
- [3] R. Panda, R. Malheiro, and R. P. Paiva, "Novel audio features for music emotion recognition," *IEEE Transactions on Affective Computing*, vol. 11, no. 4, pp. 614–626, 2020.
- [4] Y. Xiao, H. Ruan, X. Zhao, P. Jin, L. Tian, Z. Wei, X. Cai, Y. Wang, and L. Liu, "An efficient bi-modal fusion framework for music emotion recognition," *IEEE Transactions on Affective Computing*, vol. 16, no. 2, pp. 999–1015, 2025.
- [5] C. Bao and Q. Sun, "Generating music with emotions," *IEEE Transactions on Multimedia*, vol. 25, pp. 3602–3614, 2023.
- [6] Y. Wang, M. Chen, and X. Li, "Continuous emotion-based image-to-music generation," *IEEE Transactions on Multimedia*, vol. 26, pp. 5670–5679, 2024.
- [7] Q. Li, T. Zhang, C. L. P. Chen, X. Zhang, and B. Hu, "Dgc-link: Dual-gate chebyshev linkage network on eeg emotion recognition," *IEEE Transactions on Affective Computing*, vol. 16, no. 4, pp. 3499–3511, 2025.
- [8] V. S. Narayanan and A. Tarafdar, "Music therapy-driven mood-based music recommendation system integrating user emotion, song lyrics, and health reflections," in *2025 AI-Driven Smart Healthcare for Society 5.0*, 2025, pp. 19–24.
- [9] C. L. Philip Chen, B. Chen, and T. Zhang, "Adamgraph: Adaptive attention-modulated graph network for eeg emotion recognition," *IEEE Transactions on Cybernetics*, vol. 55, no. 5, pp. 2038–2051, 2025.
- [10] J. Kim and E. André, "Emotion recognition based on physiological changes in music listening," *IEEE Transactions on Pattern Analysis and Machine Intelligence*, vol. 30, no. 12, pp. 2067–2083, 2008.
- [11] X. Hu and Y.-H. Yang, "Cross-dataset and cross-cultural music mood prediction: A case on western and chinese pop songs," *IEEE Transactions on Affective Computing*, vol. 8, no. 2, pp. 228–240, 2017.
- [12] T. Greer, K. Mundrich, M. Sachs, and S. Narayanan, "The role of annotation fusion methods in the study of human-reported emotion experience during music listening," in *ICASSP 2020 - 2020 IEEE International Conference on Acoustics, Speech and Signal Processing (ICASSP)*, 2020, pp. 776–780.
- [13] J. J. Deng and C. H. Leung, "Dynamic time warping for music retrieval using time series modeling of musical emotions," *IEEE Transactions on Affective Computing*, vol. 6, no. 2, pp. 137–151, 2015.
- [14] L. Xu, X. Wen, J. Shi, S. Li, Y. Xiao, Q. Wan, and X. Qian, "Effects of individual factors on perceived emotion and felt emotion of music: based on machine learning methods," *Psychology of Music*, vol. 49, no. 5, pp. 1069–1087, 2021.
- [15] A. Sayal, A. G. Guedes, I. Almeida, D. J. Pereira, C. F. Lima, R. Panda, R. P. Paiva, T. Sousa, M. Castelo-Branco, I. Bernardino, and B. Direito, "Decoding musical valence and arousal: Exploring the neural correlates of music-evoked emotions and the role of expressivity features," *IEEE Transactions on Affective Computing*, vol. 16, no. 2, pp. 1247–1259, 2025.
- [16] A. Aljanaki, Y.-H. Yang, and M. Soleymani, "Developing a benchmark for emotional analysis of music," *PloS one*, vol. 12, no. 3, p. e0173392, 2017.
- [17] H.-T. Hung, J. Ching, S. Doh, N. Kim, J. Nam, and Y.-H. Yang, "Emopia: A multi-modal pop piano dataset for emotion recognition and emotion-based music generation," in *International Society for Music Information Retrieval Conference, ISMIR 2021*. International Society for Music Information Retrieval, 2021.

- [18] D. Turnbull, L. Barrington, D. Torres, and G. Lanckriet, "Semantic annotation and retrieval of music and sound effects," *IEEE Transactions on Audio, Speech, and Language Processing*, vol. 16, no. 2, pp. 467–476, 2008.
- [19] E. Coviello, A. B. Chan, and G. Lanckriet, "Time series models for semantic music annotation," *IEEE Transactions on Audio, Speech, and Language Processing*, vol. 19, no. 5, pp. 1343–1359, 2011.
- [20] K. Zhang, H. Zhang, S. Li, C. Yang, and L. Sun, "The pmemo dataset for music emotion recognition," in *Proceedings of the 2018 ACM on international conference on multimedia retrieval*, 2018, pp. 135–142.
- [21] Y. Wang, Y. Jing, W. Wei, D. Cazau, O. Adam, and Q. Wang, "Pipaset and teas: A multimodal dataset and annotation platform for automatic music transcription and expressive analysis dedicated to chinese traditional plucked string instrument pipa," *IEEE Access*, vol. 10, pp. 113 850–113 864, 2022.
- [22] R. Miotto and G. Lanckriet, "A generative context model for semantic music annotation and retrieval," *IEEE Transactions on Audio, Speech, and Language Processing*, vol. 20, no. 4, pp. 1096–1108, 2012.
- [23] G. Liu and Z. Tan, "Research on multi-modal music emotion classification based on audio and lyrics," in *2020 IEEE 4th Information Technology, Networking, Electronic and Automation Control Conference (ITNEC)*, vol. 1, 2020, pp. 2331–2335.
- [24] L. Turchet, B. O'Sullivan, R. Ortner, and C. Guger, "Emotion recognition of playing musicians from eeg, ecg, and acoustic signals," *IEEE Transactions on Human-Machine Systems*, vol. 54, no. 5, pp. 619–629, 2024.
- [25] X. Li, X. Shi, D. Hu, Y. Li, Q. Zhang, Z. Wang, M. Unoki, and M. Akagi, "Music theory-inspired acoustic representation for speech emotion recognition," *IEEE/ACM Transactions on Audio, Speech, and Language Processing*, vol. 31, pp. 2534–2547, 2023.
- [26] X. Han, F. Chen, and J. Ban, "Ffmfn: A fuzzy multimodal fusion network for emotion recognition in ensemble conducting," *IEEE Transactions on Fuzzy Systems*, vol. 33, no. 1, pp. 168–179, 2025.
- [27] Y. Li, Z. Zhang, J. Han, P. Bell, and C. Lai, "Semi-supervised cognitive state classification from speech with multi-view pseudo-labeling," in *ICASSP 2025 - 2025 IEEE International Conference on Acoustics, Speech and Signal Processing (ICASSP)*, 2025, pp. 1–5.
- [28] S. Huang, Z. Jin, D. Li, J. Han, and X. Tao, "Multimodal fusion for eeg emotion recognition in music with a multi-task learning framework," in *ICASSP 2025 - 2025 IEEE International Conference on Acoustics, Speech and Signal Processing (ICASSP)*, 2025, pp. 1–2.
- [29] G. Brunner, A. Konrad, Y. Wang, and R. Wattenhofer, "Midi-vae: Modeling dynamics and instrumentation of music with applications to style transfer," in *Proceedings of the 19th International Society for Music Information Retrieval Conference (ISMIR 2018)*. dblp, 2018, pp. 747–754.
- [30] T.-B. Li, Y.-T. Su, D. Song, W.-H. Li, Z.-Q. Wei, and A.-A. Liu, "Progressive fourier adversarial domain adaptation for object classification and retrieval," *IEEE Transactions on Multimedia*, vol. 26, pp. 4540–4553, 2024.
- [31] M. Soleymani, M. N. Caro, E. M. Schmidt, C.-Y. Sha, and Y.-H. Yang, "1000 songs for emotional analysis of music," in *Proceedings of the 2nd ACM International Workshop on Crowdsourcing for Multimedia*, ser. CrowdMM '13. New York, NY, USA: Association for Computing Machinery, 2013, p. 1–6.
- [32] Y.-A. Chen, Y.-H. Yang, J.-C. Wang, and H. Chen, "The amg1608 dataset for music emotion recognition," in *2015 IEEE International Conference on Acoustics, Speech and Signal Processing (ICASSP)*, 2015, pp. 693–697.
- [33] L. N. Ferreira and J. Whitehead, "Learning to generate music with sentiment," *Proceedings of the Conference of the International Society for Music Information Retrieval*, 2019.
- [34] J. S. Gómez-Cañón, N. Gutiérrez-Páez, L. Porcaro, A. Porter, E. Cano, P. Herrera-Boyer, A. Gkiokas, P. Santos, D. Hernández-Leo, C. Karrenman *et al.*, "Trompa-mer: an open dataset for personalized music emotion recognition," *Journal of Intelligent Information Systems*, vol. 60, no. 2, pp. 549–570, 2023.
- [35] X. Hu, J. S. Downie, and A. F. Ehmann, "Lyric text mining in music mood classification," *American music*, vol. 183, no. 5, 049, pp. 2–209, 2009.
- [36] G. Yin, S. Sun, D. Yu, D. Li, and K. Zhang, "A multimodal framework for large-scale emotion recognition by fusing music and electrodermal activity signals," *ACM Transactions on Multimedia Computing, Communications, and Applications (TOMM)*, vol. 18, no. 3, pp. 1–23, 2022.
- [37] Y. E. Kim, E. M. Schmidt, R. Migneco, B. G. Morton, P. Richardson, J. Scott, J. A. Speck, and D. Turnbull, "Music emotion recognition: A state of the art review," in *Proc. ismir*, vol. 86, 2010, pp. 937–952.
- [38] J. Dutta and D. Chanda, "Music emotion recognition in assamese songs using mfcc features and mlp classifier," in *2021 International Conference on Intelligent Technologies (CONIT)*, 2021, pp. 1–5.
- [39] Z. Li, F. Liu, W. Yang, S. Peng, and J. Zhou, "A survey of convolutional neural networks: Analysis, applications, and prospects," *IEEE Transactions on Neural Networks and Learning Systems*, vol. 33, no. 12, pp. 6999–7019, 2022.
- [40] A. Graves, "Long short-term memory," *Supervised sequence labelling with recurrent neural networks*, pp. 37–45, 2012.
- [41] K. Choi, G. Fazekas, M. Sandler, and K. Cho, "Convolutional recurrent neural networks for music classification," in *2017 IEEE International Conference on Acoustics, Speech and Signal Processing (ICASSP)*, 2017, pp. 2392–2396.
- [42] A. Amjad, S. Khuntia, H.-T. Chang, and L.-C. Tai, "Multi-domain emotion recognition enhancement: A novel domain adaptation technique for speech-emotion recognition," *IEEE Transactions on Audio, Speech and Language Processing*, vol. 33, pp. 528–541, 2025.
- [43] J. Quilingking Tomas, R. A. S. Jamilla, K. S. Lopo, and C. E. Camba, "Multimodal emotion detection model implementing late fusion of audio and lyrics in filipino music," in *Proceedings of the 2020 3rd International Conference on Computing and Big Data*, 2020, pp. 78–84.
- [44] J. Zhao and K. Yoshii, "Multimodal multifaceted music emotion recognition based on self-attentive fusion of psychology-inspired symbolic and acoustic features," in *2023 Asia Pacific Signal and Information Processing Association Annual Summit and Conference (APSIPA ASC)*, 2023, pp. 1641–1645.
- [45] C. Chen and Q. Li, "A multimodal music emotion classification method based on multifeature combined network classifier," *Mathematical Problems in Engineering*, vol. 2020, no. 1, p. 4606027, 2020.
- [46] Z. Li, E. Zhu, M. Jin, C. Fan, H. He, T. Cai, and J. Li, "Dynamic domain adaptation for class-aware cross-subject and cross-session eeg emotion recognition," *IEEE Journal of Biomedical and Health Informatics*, vol. 26, no. 12, pp. 5964–5973, 2022.
- [47] A. Gabrielsson, "Emotion perceived and emotion felt: Same or different?" *Musicae scientiae*, vol. 5, no. 1_suppl, pp. 123–147, 2001.
- [48] E. Schubert, "Emotion felt by the listener and expressed by the music: literature review and theoretical perspectives," *Frontiers in psychology*, vol. 4, p. 837, 2013.
- [49] W.-L. Zheng and B.-L. Lu, "Investigating critical frequency bands and channels for EEG-based emotion recognition with deep neural networks," *IEEE Transactions on Autonomous Mental Development*, vol. 7, no. 3, pp. 162–175, 2015.
- [50] Q. Li, T. Zhang, C. L. P. Chen, K. Yi, and L. Chen, "Residual GCB-Net: Residual graph convolutional broad network on emotion recognition," *IEEE Transactions on Cognitive and Developmental Systems*, vol. 15, no. 4, pp. 1673–1685, 2023.
- [51] J. Jin, R. Xu, I. Daly, X. Zhao, X. Wang, and A. Cichocki, "Mocnn: A multiscale deep convolutional neural network for erp-based brain-computer interfaces," *IEEE Transactions on Cybernetics*, vol. 54, no. 9, pp. 5565–5576, 2024.
- [52] M. Xiao, Z. Zhu, K. Xie, and B. Jiang, "Meeg and at-dggn: Improving eeg emotion recognition with music introducing and graph-based learning," in *2024 IEEE International Conference on Bioinformatics and Biomedicine (BIBM)*, 2024, pp. 4201–4208.
- [53] N. T. Pham, D. N. M. Dang, N. D. Nguyen, T. T. Nguyen, H. Nguyen, B. Manavalan, C. P. Lim, and S. D. Nguyen, "Hybrid data augmentation and deep attention-based dilated convolutional-recurrent neural networks for speech emotion recognition," *Expert Systems with Applications*, vol. 230, p. 120608, 2023.
- [54] N. He and S. Ferguson, "Music emotion recognition based on segment-level two-stage learning," *International Journal of Multimedia Information Retrieval*, vol. 11, no. 3, pp. 383–394, 2022.
- [55] P.-C. Chang, Y.-S. Chen, and C.-H. Lee, "Iiof: Intra-and inter-feature orthogonal fusion of local and global features for music emotion recognition," *Pattern Recognition*, vol. 148, p. 110200, 2024.
- [56] Z. Huang, S. Ji, Z. Hu, C. Cai, J. Luo, and X. Yang, "Adff: Attention based deep feature fusion approach for music emotion recognition," in *Proc. Interspeech 2022*, 2022, pp. 4152–4156.
- [57] Y. Xu, H. Chen, J. Yu, Q. Huang, Z. Wu, S.-X. Zhang, G. Li, Y. Luo, and R. Gu, "Secap: Speech emotion captioning with large language model," in *Proceedings of the AAAI Conference on Artificial Intelligence*, vol. 38, no. 17, 2024, pp. 19 323–19 331.
- [58] T. Zhang, Q. Li, X. Yang, and C. L. P. Chen, "Mcgc-net: Multi-scale controllable graph convolutional network on music emotion recognition," *IEEE Transactions on Affective Computing*, pp. 1–14, 2025.



Qilin Li (Student Member, IEEE) received the B.Eng. degree in electrical engineering and automation from Wuhan University of Science and Technology, at Wuhan, China, in 2018, and the M.S. degree in computer science from University of Wollongong, at Wollongong, NSW, Australia, in 2020. He is currently pursuing the Ph.D. degree in computer science and technology with the Guangdong Provincial Key Laboratory of Computational AI Models and Cognitive Intelligence, the School of Computer Science and Engineering, South China

University of Technology, at Guangzhou, China.

His current research interests include affective computing and neural network.



C. L. Philip Chen (Life Fellow, IEEE) received the M.S. degree in electrical and computer science from the University of Michigan at Ann Arbor, Ann Arbor, MI, USA, in 1985, and the Ph.D. degree in electrical and computer science from Purdue University, West Lafayette, in USA, in 1988.

He is the Chair Professor and the Dean of the School of Computer Science and Engineering, South China University of Technology, Guangzhou, China. Being a Program Evaluator of the Accreditation Board of Engineering and Technology Education in the U.S., for computer engineering, electrical engineering, and software engineering programs, he successfully architects the University of Macau's Engineering and Computer Science programs receiving accreditations from Washington/Seoul Accord through Hong Kong Institute of Engineers (HKIE), Hong Kong, of which is considered as his utmost contribution in engineering/computer science education for Macau as the former Dean of the Faculty of Science and Technology. His current research interests include cybernetics, systems, and computational intelligence.

Dr. Chen was a recipient of the 2016 Outstanding Electrical and Computer Engineers Award from his alma mater, Purdue University in 1988. He received the IEEE Norbert Wiener Award in 2018 for his contribution in systems and cybernetics, and machine learning. He is also a highly cited researcher by Clarivate Analytics from 2018 to 2023. He is currently the Editor-in-Chief of the IEEE TRANSACTIONS ON CYBERNETICS, an Associate Editor of the IEEE TRANSACTIONS ON ARTIFICIAL INTELLIGENCE, and IEEE TRANSACTIONS ON FUZZY SYSTEMS. He was the IEEE Systems, Man, and Cybernetics Society President from 2012 to 2013, the Editor-in-Chief of the IEEE TRANSACTIONS ON SYSTEMS, MAN, AND CYBERNETICS: SYSTEMS from 2014 to 2019. He was the Chair of TC 9.1 Economic and Business Systems of International Federation of Automatic Control from 2015 to 2017. He is a Fellow of AAAS, IAPR, CAA, and HKIE; a member of Academia Europaea, European Academy of Sciences and Arts.



Tong Zhang (Senior Member, IEEE) received the B.S. degree in software engineering from Sun Yat-sen University, at Guangzhou, China, in 2009, and the M.S. degree in applied mathematics from University of Macau, at Macau, China, in 2011, and the Ph.D. degree in software engineering from the University of Macau, at Macau, China in 2016. Dr. Zhang currently is a professor and Associate Dean of the School of Computer Science and Engineering, South China University of Technology, China.

His research interests include affective computing, evolutionary computation, neural network, and other machine learning techniques and their applications. Prof. Zhang is the Associate Editor of the IEEE Transactions on Affective Computing, IEEE Transactions on Computational Social Systems, and Journal of Intelligent Manufacturing. He has been working in publication matters for many IEEE conferences.